Environ Monit Assess (2020) 192: 274
https://doi.org/10.1007/s10661-020-8220-7

Nutrient pollutant loading and source apportionment along a Mediterranean river

Sania El-Nakib · Ibrahim Alameddine · May Massoud · Majdi Abou Najm

Received: 10 September 2019 / Accepted: 17 March 2020 / Published online: 8 April 2020

Abstract Rivers are increasingly being subjected to increased anthropogenic pollution stresses that undermine their designated uses and negatively affect sensitive coastal regions. The degradation of river water quality is attributed to both point and nonpoint sources of pollution. In this study, we determine the relative contribution of point and nonpoint pollutant loads in the Beirut River basin, a poorly monitored seasonal Mediterranean river. Water quality samples were collected on a weekly basis over 2 consecutive years (2016 and 2017) from four sampling sites that represent a gradient of increasing urbanization. Flow-concentration models were first developed to estimate total phosphorus (TP), total nitrogen (TN), and total suspended solids (TSS) loads reaching the different sub-basins. The performance of the regression models varied by location and by pollutant, with improved performance in the downstream sections (adjusted R^2 66% for TP and 59% for TN). Loads were also determined using the Beale's ratio method, which generally underestimated the loads as compared with the regression-based models. The relative contribution of the nonpoint source loads were then quantified using the Open Nonpoint Source Pollution and Erosion Comparison Tool (OpenNSPECT). The results showed that point sources were the main cause of water quality impairment across the entire basin, with load contributions varying between 75% in the headwaters and 98% in the urbanized downstream sections. The adopted modeling approach in this study provides an opportunity to better understand pollutant load dynamics in poorly monitored basins and a mechanism to apportion pollution loads between point and nonpoint sources.

Keywords Water quality · Load estimation · Point sources · Nonpoint sources · Beirut River · OpenNSPECT

S. El-Nakib · I. Alameddine (✉)
Department of Civil and Environmental Engineering, Maroun Semaan Faculty of Engineering and Architecture, American University of Beirut, P.O. Box 11-0236, Riad el Solh, Beirut 1107 2020, Lebanon
e-mail: ia04@aub.edu.lb

M. Massoud
Department of Environmental Health, American University of Beirut, Bliss Street, Beirut, Lebanon

M. Abou Najm
Department of Land, Air and Water Resources, University of California Davis, One Shields Avenue, Davis, CA, USA

Introduction

Anthropogenic activities are increasingly responsible for modifying nutrient cycles in freshwater bodies (Carpenter et al. 2011; Balter 2013). Worldwide freshwater systems have been negatively affected by the pollutant discharge of land-based sources (Da Silva and Sacomani 2001; Meybeck 2003; Vörösmarty et al. 2005; Vörösmarty et al. 2010). Surface water bodies, especially in developing countries, are often used as the final destination for the discharge of wastes. According to the United Nations, around 90% of domestic wastewater and 70% of industrial wastes are discharged untreated into the water bodies of developing countries

(UN 2003). Additionally, anthropogenic-induced changes at the landscape scale have been shown to threaten the ecological integrity and water quality of many freshwater systems (Wang et al. 2016; Strayer et al. 2003; Turner and Rabalais 2003).

Streams and rivers are one of the most anthropogenically affected ecosystems (Strayer et al. 2003). Rivers provide key environmental services that include the provision of water for drinking, irrigation, and industrial purposes; transportation; food and fiber; hydropower generation and thermoelectric cooling; recreation and esthetic appreciation; nutrient cycling; as well as habitats for invertebrates, fish, amphibian, and mammals (Rissman and Carpenter 2015; Auerbach et al. 2014). Nevertheless, their status is often impaired by their poor water quality (Chapman 1996). Riverine pollutant loads are also a main driver of coastal hypoxia and eutrophication (Diaz 2001; Scavia and Bricker 2006; Rabalais et al. 2009). Pollution transport and retention mechanism in Mediterranean rivers are poorly characterized as compared with temperate river (López-Doval et al. 2013; Bernal et al. 2013). Malagó et al. (2019) estimated that Mediterranean rivers were responsible for delivering 1.87 Tg/year and 0.11 Tg/year of total nitrogen and total phosphorus to the Mediterranean Sea, respectively. These loads have caused severe eutrophication of coastal regions, particularly along the Eastern Mediterranean Sea, which is ultraoligotrophic and is the largest phosphorus limited water body in the world (Karydis and Kitsiou 2012). While our overall knowledge of the quantities and quality of pollutants in Mediterranean rivers remain limited, the chemical and ecological status of most rivers in the southeastern Levantine basin remains unknown due to poor monitoring (López-Doval et al. 2013). These systems tend to be dominated with intermittent rivers and streams that are extremely sensitive to hydrological and anthropogenic pressure (Kalogianni et al. 2017). The extreme seasonal and interannual variability in flow, the large withdrawals of water as a result of increased demands in these water scarce regions, and changes in the river's connectivness have been found to increase the pollution risks from these rivers and affect nutrient dynamics (López-Doval et al. 2013; Bernal et al. 2013; A. Alberto et al. 2016). Thus, establishing a better understanding and a quantification of the sources and sinks of nitrogen and phosphorus in Mediterranean rivers is critical toward guiding river basin management plans and protecting coastal ecosystems (Malagó et al. 2019).

Environmental regulations have been promulgated worldwide to limit and control the sources of river water pollution such as the TMDL program initiated in the 1972 Clean Water Act in the USA (National Research Council 2001) and the European Water Framework Directive (Borja et al. 2006; Yang and Wang 2010). The implementation of these measures has resulted in a significant reduction in point source pollution in most developed countries and the subsequent improvement in the quality of lakes, rivers, reservoirs, groundwater, and coastal waters; yet efforts aimed at controlling nonpoint sources of pollution have not been as successful (National Research Council 2001). Diffuse sources of pollution, originating from agricultural runoffs and urban surfaces, remain a significant source of impairment across many freshwater systems (Schoumans et al. 2014).

The successful implementation of an effective river management plan is contingent on the estimation of the pollutant loads and the identification and quantification of their sources (Novotny 2003; Ding et al. 2014; Pellerin et al. 2014; Novotny 1999; Rissman and Carpenter 2015; Granger et al. 2010). Estimating pollutant loads is often associated with uncertainties introduced by the limited frequency of water quality sampling, the adopted sampling method, and the duration of the monitoring campaign (Cha et al. 2010; Littlewood et al. 1998; Salles et al. 2008; Littlewood and Marsh 2005; Ullrich and Volk 2010). These uncertainties are more pronounced for small rivers (Harmel and King 2005; Ullrich and Volk 2010). Different load estimation methods have been developed; these include (1) variants of regression-based analysis (Ferguson 1986; Cohn et al. 1989; Runkel et al. 2004; Hirsch et al. 2010; Quilbé et al. 2006; Alameddine et al. 2011; Elwan et al. 2018; Efthimiou 2019), (2) ratio estimators (Cha et al. 2010; Littlewood et al. 1998; Phillips et al. 1999; Moatar et al. 2006; Salles et al. 2008; Elwan et al. 2018), and (3) interpolation techniques (Littlewood et al. 1998; Littlewood 1995; Phillips et al. 1999; Richards and Holloway 1987; Preston et al. 1989; Moatar and Meybeck 2005). Moreover, water quality models are used to identify and estimate the different sources of pollutants entering a water body. These models range from empirical models such as land use/land cover regression-based models (Wang et al. 2016) to semiempirical models the likes of the SPAtially Referenced Regressions On Watershed attributes (SPARROW) model, the Geospatial Equation for European Nutrient losses (GREEN) model (Grizzetti et al. 2005), and the Source Load Apportionment Model (SLAM) (Mockler et al. 2016), to mechanistic (or physical-based) models such as the Soil Water and Analysis Tools (SWAT) (Srinivasan and Arnold 1994).

In this study, the water quality and flow of a seasonal Mediterranean river, namely, the Beirut River, were monitored and assessed over 2 years. Pollutant loads of total nitrogen (TN), total phosphorus (TP), and total suspended solids (TSS) were then quantified at different sections of the river. Additionally, the calculated pollution loads were apportioned into point and nonpoint sources by the use a geospatial model. Correlations between the land cover of the monitored sub-watersheds and the measured river water quality were also explored. This study is the first study of its kind to be done on a seasonal Mediterranean river. It is hoped that this work will both provide a better understanding of pollutant fluxes from small seasonal Mediterranean basins while also supporting decision-makers to take the necessary measures needed to protect these important natural resources from anthropogenic point and non-point pollution.

Materials and methodology

Study area

The Beirut River springs from the western slopes of Mount Lebanon at an altitude of 1890 m. The river flows westward for about 20 km before discharging into the Mediterranean Sea. Its watershed has a total area of 228 km^2, which is considered large for coastal Mediterranean basins, whose areas rarely exceed 100 km^2 (Salles et al. 2008). Around 200,000 inhabitants reside within the boundaries of the Beirut River. Like many Mediterranean rivers, the Beirut River is seasonal. The Mediterranean climate, with its marked contrasts between the dry and wet seasons, increases the difficulty of pollutant load estimation (Salles et al. 2008; Tzoraki et al. 2014). The land use/land cover (LULC) of the watershed changes with elevation. The headwaters of the basin are covered by dense forests, while the lower sections are industrialized and rapidly urbanizing. In this work, four sampling stations were selected along the Beirut River. The locations of the sampling stations are represented in Fig. 1. Based on the adopted 4 sampling stations, the Beirut River was subdivided into five sub-catchments (Fig. 1), two of which are headwaters (S1B and S2B). Table 1 describes the LULC for each of the five sub-catchments.

Water quality sampling

The water quality sampling stations were chosen to cover a wide range of LULCs within the watershed. The sampling was conducted between April 2016 and November 2017. Weekly grab samples from the four stations were collected when the river was flowing. Temperature, pH, and conductivity measurements were performed on site. Moreover, collected water quality samples were stored at 4 °C and transported for further laboratory analysis (Table 2). Microbiological tests were also conducted to assess the total and fecal coliform concentrations at the four sites. Note that while grab samples may not provide a complete picture of pollutant dynamics as compared with campaigns based on high-resolution sensors (Rozemeijer et al. 2010; Vandenberghe et al. 2005), the former will continue to be the backbone of monitoring programs in the foreseeable future due to financial and technical constraints (Jomaa et al. 2018; Ullrich and Volk 2010). In this study, we focused on quantifying the TN, TP, and TSS loads. The estimation and source apportionment of bacterial loads were initially planned; yet both fecal and total coliform concentrations were found to be too numerous to count across the 4 sampling locations, even when 1:100 dilution was attempted.

Flow measurements

Flow measurements for the Beirut River were provided by the Litani River Authority (LRA) at three sampling stations (S2, S3 and S4 in Fig. 1), while the flow at S1 was measured concurrently with the water quality sampling program using an electromagnetic flow meter (a Hach FH950 flow meter). Flows were estimated based on the ISO 748:2007 standards for the midsection method. Note that a regression equation was developed to estimate the flow at S1 from the flow recorded at S2 (Eq. 1). Regression models have been shown to be successful in estimating daily tributary flows in ungauged sub-catchments based on flow data from other gauging stations within the same catchment (Reinelt and Grimvall 1992). The model was able to predict 80% of the variability in the observed flow at S1 (El-Nakib et al. 2018).

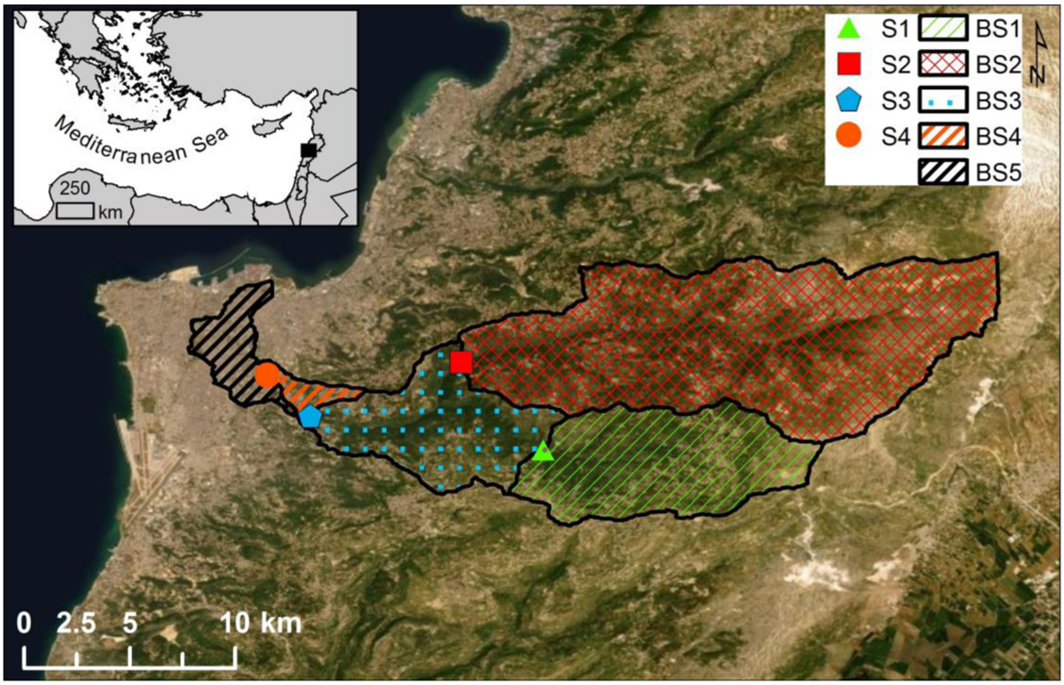

Fig. 1 Map of the Beirut River sub-catchments and locations of sampling stations

$$\sqrt{Q_{S1} = 0.25 + 0.55\sqrt{Q_{S2}} + \cos\left(\frac{2\pi T_{sample}}{365}\right); \varepsilon} \qquad (1)$$

where $\sqrt{Q_{S1}}$ is the square root of measured flow at S1, *cos* ($2\pi Tsample/365$) is the seasonal factor determined as a function of the cosine of the time of sampling, T_{sample} is the sampling date starting (i.e., April 1 2016 = 1), and ε is the residual error of the model; ε~N(0, 0.21).

Load estimation

Pollutant load estimation

Pollutant loads were estimated based on data collected from the in situ water quality monitoring and flow measurements from the three existing gauging stations (S2, S3, and S4). Given that water quality data are often limited as compared with flow data, flow-concentration relationships were developed in an effort to estimate total pollutant loads and impute missing pollutant concentration (Bowes et al. 2008; Dolan et al. 1981; Koch and Smillie 1986; Ferguson 1987; Phillips et al. 1999; Haggard et al. 2003; Malan and Day 2003; Smith and Croke 2005; Pellerin et al. 2014). Statistical approaches, such as regression models, are typically used to estimate missing pollutant concentrations. This is done through the development of regression-based models that predicts pollutant concentration from flow data (Dolan et al. 1981; Cohn 1995; Richards 1998; Park and Engel 2014; Ferguson 1986; Cohn et al. 1989; Runkel et al. 2004; Hirsch et al. 2010; Quilbé et al. 2006;

Table 1 General description of the five sub-catchments of the Beirut River

Sub-catchment	Sub-catchment area (km^2)	Population	Dominant land uses (% area)
BS1	49	13,000	Forest: 50%; Agriculture: 7%; Urban: 10%; Other: 33%
BS2	126	32,000	Forest: 57%; Agriculture: 11%; Urban: 5%; Other: 27%
BS3	37	26,500	Forest: 67%; Agriculture: 8%; Urban:12%; Other: 13%
BS4	4	11,750	Forest: 28%; Agriculture: 19%; Urban: 47%; Other: 6%
BS5	11.5	116,000	Forest: 4%; Agriculture: 9.5%; Urban: 72%; Other: 14.5%

Table 2 Adopted water quality analysis methods (Rice et al. 2012)

	Quality indicators	Method	Method number
Physical	pH	Electrometery	4500-H + B
	Conductivity	Electrometery	9050-A
	Total suspended solids (TSS)	Filtration	2540-B
Chemical	Chemical oxygen demand	Reactor digestion	5220-D
	Biochemical oxygen demand	Respirometry	5210-B
	TN (Total nitrogen)	TNT persulfate digestion	10071
	TP (Total phosphorus)	Acid persulfate digestion	4500-P.B&E
	Sulfate	Spectrophotometrically	10200 H.2
Microbiological	TC/FC (Total coliform/fecal coliform)	Membrane filtration	9222B/9222D

Alameddine et al. 2011; Elwan et al. 2018; Efthimiou 2019). The functional form of these flow-concentration models is often represented by single or multiple linear regression equations with logarithmic transformation (Gilroy et al. 1990; Brezonik and Stadelmann 2002). In this study, multiple linear regression models were developed at each station to predict the TN, TP, and TSS pollutant concentrations as a function of the flow measurements, water temperature, and seasonality (Eq. 2) (Lee et al. 2016; Haggard et al. 2003). Regression models were fit using the R software (R Core Team 2017) based on the stepwise selection procedure that eliminates insignificant variables. The best models were chosen based on Akaike's Information Criteria (AIC) (Akaike 1974), with the lowest AIC value indicating the most parsimonious model.

$$\begin{aligned} Trans(C_x) &= \beta_0 + \beta_1 \log(Q) + \beta_2 \left(\log\left(Q\right)\right)^2 \\ &\quad + \beta_3 \cos(2\pi T/365) \\ &\quad + \beta_4 \sin(2\pi T/365) + \beta_5 (Temp) + \varepsilon \quad (2) \end{aligned}$$

where $Trans(C_x)$ is the transformed concentration for each pollutant (x: TP, TN, or TSS) where both natural logarithm and square root transformations were used, $\log(Q)$ is the logarithmic transformation of flow (m^3/s), $\cos\left(\frac{2\pi T}{365}\right)$ is the seasonal factor determined as a function of the cosine of the time of sampling, T is the sampling start date (i.e., April 1 2016 = 1), $\sin\left(\frac{2\pi T}{365}\right)$ is the seasonal factor determined as a function of the sine of the time of sampling, T is the sampling date starting, $Temp$ is the temperature in °C, and ε is the residual error of the model; $\varepsilon \sim \mathrm{Norm}(0, \sigma^2)$.

The total annual TP, TN, and TSS loads were then estimated by summing the daily loads as shown in Eq. 3. The uncertainty in the regression-based load predictions was quantified using a Monte Carlo simulation. The predictive distribution of each of the pollutant concentrations was described by a conditional normal distribution with a mean given by the simulated coefficients of each variable and the simulated standard error from each linear model. The Monte Carlo simulations were done using the sim function in the arm package in R (Gelman et al. 2016). Ten thousand simulations were conducted for each flow measurement. The function returns a vector of simulated residual standard deviations and a matrix of simulated regression coefficients. We used these simulations to generate the predictive distribution for each pollutant. These distributions account for the model uncertainties in the multiple regression model. Note that the use of Monte Carlo simulations helps address retransformation biases (Qian 2016).

$$\widehat{L}_\tau = \Delta t \sum_{i=1}^{NP} \widehat{L}_i = \Delta t \sum_{i=1}^{NP} \left(Q\widehat{C}\right)_i \quad (3)$$

where $\widehat{L}_\tau$ is the estimate of total pollutant load, $\widehat{L}_i$ is the estimate of instantaneous load, NP is the number of discrete points in time when $Q > 0$, and Δt is the time interval represented by instantaneous load (1 day).

The Beale's ratio (BR) estimator method was also used to estimate pollutant loads (Eqs. 4 and 5). This method has been reported to outperform the regression-based approach when the flow-concentration relationship is not log linear and/or it has high variance (Preston et al. 1989). Quilbé et al. (2006) has also recommended its use when the available concentration data are limited as compared with the flow data. Nevertheless, the BR method has been shown to require a larger number of samples as compared with the regression method to achieve the same level of accuracy (Preston et al. 1989; Richards and Holloway 1987; Lee et al. 2016). The BR load estimation approach has been utilized extensively in the estimation of pollutant loads in the Great Lakes area and other regions of the USA (Richards and Holloway 1987; Cha et al. 2010; Dolan et al. 1981). Quilbé et al. (2006) and Elwan et al. (2018) also used the ratio estimator method to calculate sediment and nutrient loads in the watersheds of the Beaurivage River in Quebec, Canada, and the Manawatu River in New Zealand, respectively. The Beale's method estimates the total pollutant loads by summing up the daily sampled loads with the product of the estimated Beale's ratio multiplied by the total flow for all days when the pollutants were not sampled and for which there was a flow measurement (Eq. 5).

$$BR = \widehat{R}\left(\frac{1+\frac{1-f}{n}c_{LQ}}{1+\frac{1-f}{n}c_{QQ}}\right) \tag{4}$$

where $\widehat{R} = \bar{l}\Big/\bar{q}$ is the ratio of the sample means of load and flow; $f = {}^{n}/_{N}$ is the ratio of the number of samples, n, to the total number of days (sampled or unsampled) in the prediction period, N (when Q > 0); $c_{\mathrm{LQ}} = {}^{s_{LQ}}/_{(\bar{l}\,\bar{q})}$ is the ratio of the sample covariance between load and flow,s_{LQ}, to the product of the sample means of load and flow; and $c_{QQ} = {}^{s_Q^2}\Big/_{\bar{q}^2}$ is the ratio of the sample variance of flow to the square of the sample mean of flow

$$L_t = \sum_{i=1}^{n} C_i \times Q_i + BR \times \sum_{j=n+1}^{NP} Q_j \tag{5}$$

The mean squared error (MSE) around the estimated mean daily load was calculated using Eq. 6 (Richards 1998). Note that the MSE is equivalent to the variance of the estimated daily load given that the bias is negligible, as it approximately varies as a function of $1/n^2$ (Tin 1965).

$$Var = \bar{l}_o^2\left[\left(\frac{1}{n}-\frac{1}{N}\right)\left(\frac{s_Q^2}{\bar{q}^2}+\frac{s_L^2}{\bar{l}^2}-2\frac{s_{LQ}}{\bar{l}\,\bar{q}}\right)+\left(\frac{1}{n}-\frac{1}{N}\right)^2\left(2\frac{s_Q^4}{\bar{q}^4}-4\frac{s_Q^2\times s_{LQ}}{\bar{q}^2\times\bar{l}\,\bar{q}}+\frac{s_{LQ}^2}{\left(\bar{l}\,\bar{q}\right)^2}+\frac{s_Q^2\times s_L^2}{\bar{q}^2\times\bar{l}^2}\right)\right] \tag{6}$$

where s_L^2 is the variance of measured daily loads.

Parametric t-tests on the log-transformed loads were conducted to assess for statistical differences between the two pollutants load estimation methods used. Furthermore, the Levene's test was conducted to assess for statistical differences in the variances estimated by each of the two methods. Note that these statistical tests were conducted at the 95% confidence level ($\alpha = 0.05$) and were performed using the R software (R Core Team 2017).

Nonpoint source load estimation: OpenNSPECT model

Nonpoint source pollutant loads contribute part of the total pollutant loads reaching the river. The OpenNSPECT model was used to estimate the annual TP, TN, and TSS nonpoint loads reaching the Beirut River. The OpenNSPECT software is a model developed by the National Oceanic and Atmospheric Administration (NOAA) Office for Coastal Management to examine nonpoint pollution loads at the watershed level based on the land use/land cover, elevation, soil types, precipitation, and adopted best practices. The model has been successfully used to assess the effect of land use modifications in several places in the USA, including the Deep River watershed area in Indiana and Ko'olaupoko in Hawaii (Viswanathan and Karim 2015). OpenNSPECT has also been used to assess the effects of wildfire on nonpoint source pollutants reaching sensitive oceanic ecosystems (Morrison and Kolden 2015). Moreover, the model has been used to recommend nonpoint source management practices in several areas with high levels of pollutant (KBAC 2007). The model estimates nonpoint pollutant loads (TN, TP, and TSS) by generating pollutant concentration grids from assigned load contribution coefficients based on land cover classes (Table 3).

Water routing for the model was based on a 10 m Digital Elevation Model (DEM) for the watershed that was provided by the Department of Geographic Affairs in the Lebanese Army. Flow direction, flow accumulation, length slope (Eq. 7), and watershed boundary delineation were conducted using ESRI's Spatial Analyst toolbox under ArcGIS 10.5.1. Moreover, maps for the erodibility factor (*k*) and the hydrologic soil groups were generated based on the 2006 national soil map developed by the Lebanese National Center for Scientific Research (Darwish 2006).

$$ls = \left(\frac{[Flowacc]*resolution}{22.1}\right)^{0.4} * \left(\frac{\sin([slope]*0.01745)}{0.09}\right)^{1.4} *1.4 \qquad (7)$$

where *Flowacc* is the the accumulated flow into each cell, *resolution* is the cell resolution (10 m in this study), and *slope* is the rate of maximum change in the *z*-direction generated for each cell from the raster surface (DEM). The slope raster in degrees was calculated using the slope tool under Spatial Analyst toolbox in ArcGIS 10.5.1.

OpenNSPECT predictions include both an accumulated and local effect grids. These grids present the mobilization and accumulation of pollutants through the landscape as well as the amounts of pollutants originating from each cell in the watershed area. These grids include the accumulated runoff, pollutant concentration, accumulated pollutant loads, runoff local effect, and pollutant local effect (NOAA 2012).

Results and discussion

Measured TN and TP concentrations across both seasons consistently exceeded the nutrient criteria that are recommended by the USEPA for rivers in xeric environments (Ecoregion III) (USEPA 2000) (Table 4). The water quality in the Beirut River also showed strong seasonality. Observed pollutant levels in the wet season tended to be lower across the four stations due to dilution. Similar observations have been recorded in other point source dominated river systems (Chang 2008; Massoud et al. 2006; Vega et al. 1998; W. D. Alberto et al. 2001). Throughout the year, the levels of TN and TP concentrations exhibited a significant negative relationship with river flow across the three monitoring stations (S1, S3, and S4). This indicates that pollutant dilution rather than pollutant wash-off is the dominating process controlling pollutant loading into these sub-basins (SB1, SB3, and SB4). This negative relationship between flow and concentration also suggests the dominance of point source pollution sources as compared with nonpoint sources. At station S2, the dilution effect was less apparent as the correlation between flow and pollutant concentrations was weak. Possibly, this is attributed to SB2 having the lowest population density and percent urban cover as well as the highest forest cover among the four sampled sub-basins in the river.

Total pollutant load estimation

Regression-based method

The application of the regression-based approach was only possible for the estimation of TN and TP loads at S1, S3, and S4. No statistically significant relationship between TN and TP concentrations on one hand and flow on the other were found at S2. Moreover, the correlation between TSS and flow proved to be weak across all stations, and as such no significant regression models could be fit. The lack of significant correlations with flow suggests the lack of a dominant source and/or extensive pollutant processing within the affected sub-catchments (Tappin et al. 2013). Table 4 summarizes the regression equations developed for the estimation of the daily TN and TP pollutant concentrations by station.

Table 3 Pollutant coefficients for the given land cover classes (NOAA 2014)

Land cover class	Total nitrogen (mg/L)	Total phosphorus (mg/L)	Total suspended solids (mg/L)
Water	0.00	0.00	0.00
High intensity developed	2.22	0.47	71.00
Bare land	0.97	0.12	70.00
Mixed forest	1.25	0.05	11.00
Sedge herbaceous	0.00	0.00	0.00
Cultivated land	2.68	0.42	55.30

The adjusted R^2 of the regression models at station S1 was around 40%. For TN, the model predicted that the median concentrations at S1 were expected to decrease by around 4% for every 10% increase in flow. For TP levels, the model predicted that for every 10% increase in flow, the median TP concentrations were expected to drop by 5.3%. Moving downstream to station S3, the regression model for TN concentration was capable of explaining around 30% of the observed variability in concentrations. The model predicted that for every 10% increase in stream flow, the TN concentration was expected to drop on average by 2.1%. For TP concentrations at S3, the model was able to explain around 58% of the variance in the data. Finally, the regression models at station S4 for both TN and TP were found to be a function of flow and seasonality. The lowest and highest TN concentrations were expected to occur in April and in October, respectively. As for the effect of flow, the model predicts that for every 10% increase in flow, the TN concentrations were expected to drop by 3.3%. The TN model for S4 had an adjusted R^2 of 60%. For the TP regression model at S4, the model structure showed a significant interaction between flow and season. The model was able to explain 66% of the variability observed in the data. The overall performance of the regression-based models as compared with observational data can be seen in Fig. 2. Overall, the regression models appear to provide reasonable estimates of the observed concentrations.

Making use of the regression equations established for TN and TP at S1, S3, and S4, 10,000 simulations of daily pollutant concentration realizations were generated over the sampling period per station. These simulations were then used to generate predictive distributions for the annual TN and TP loads at S1, S3, and S4 (Fig. 3). Estimates of the total annual TN and TP loads across the stations showed that the highest loads were expected downstream at S4, while the smallest loads were upstream at S1. The median annual TN load at S4 was approximately 12 times higher than the estimated median load at S1. As for the TP annual load estimates, a 600% increase in the median total load was expected while moving downstream from the northern uppermost station (S1) to the most downstream station (S4). It is also worth mentioning that the estimated TN total annual loads were at least one order of magnitude higher than the estimated TP total loads across the three stations.

Beale's ratio-based method

Similar to the regression-based analysis, the Beale's ratio results showed that all pollutant loads exhibited an increasing trend moving from the upstream to the downstream sections of the river (Table 5). The highest mean TN load was recorded at S4, and it was around 10 times larger than that estimated at S1. In addition, the mean TP load at S4 was around 3 times larger than the mean load estimated at S1. Similarly, TSS loads were found to increase as one moved from the upstream sections of the river down to the downstream stations. This is largely due to the fact that the headwaters of the river are still heavily forested, which protects against soil erosion.

Table 4 Measured concentrations of TN and TP across the 4 stations in the dry and wet seasons

Station	Season	TN		TP	
		Mean (± 1 sd)	% Exceedance [a]	Mean (± 1 sd)	% Exceedance [a]
S1	Dry	8.90 (5.80)	100	0.69 (0.47)	100
	Wet	2.00 (1.17)	87	0.29 (0.23)	93
S2	Dry	ND	ND	ND	ND
	Wet	3.15 (2.96)	91	0.25 (0.14)	91
S3	Dry	13.18 (4.46)	100	1.92 (0.73)	100
	Wet	3.82 (2.67)	93	0.37 (0.37)	93
S4	Dry	18.72 (6.82)	100	1.73 (1.9)	100
	Wet	4.17 (3.28)	94	0.45 (0.36)	94

ND: No data as the river was dry during the dry season at Station S2

[a] Exceedance was based on the proposed nutrient criteria defined for rivers in xeric environments (Ecoregion III). TN criteria =0.38 mg/L; TP criteria 21.88 μg/L (USEPA 2000)

Comparison between the regression-based loads and the Beale's ratio loads

Differences between the total pollutant loads estimated by the regression-based method and those based on the Beale's ratio are shown in Fig. 4. Overall, the predicted mean TN and TP annual loads at S1, S2, and S4 for both methods were found to be within the same order of magnitude. Yet, their means were still found to be statistically different (p value < 0.05), with the exception of TP at S3 (p value = 0.08). This is in agreement with the conclusions of Lee et al. (2016), who also reported statistically significant differences between the load estimation methods across several rivers and streams in the continental USA. It is worth mentioning that the regression-based estimates consistently overpredicted as compared with the Beale's estimates across all stations except for the TP load at S3 (Fig. 4). This could be attributed to the seasonal variation in pollutant concentrations, which can cause heteroscedasticity in the

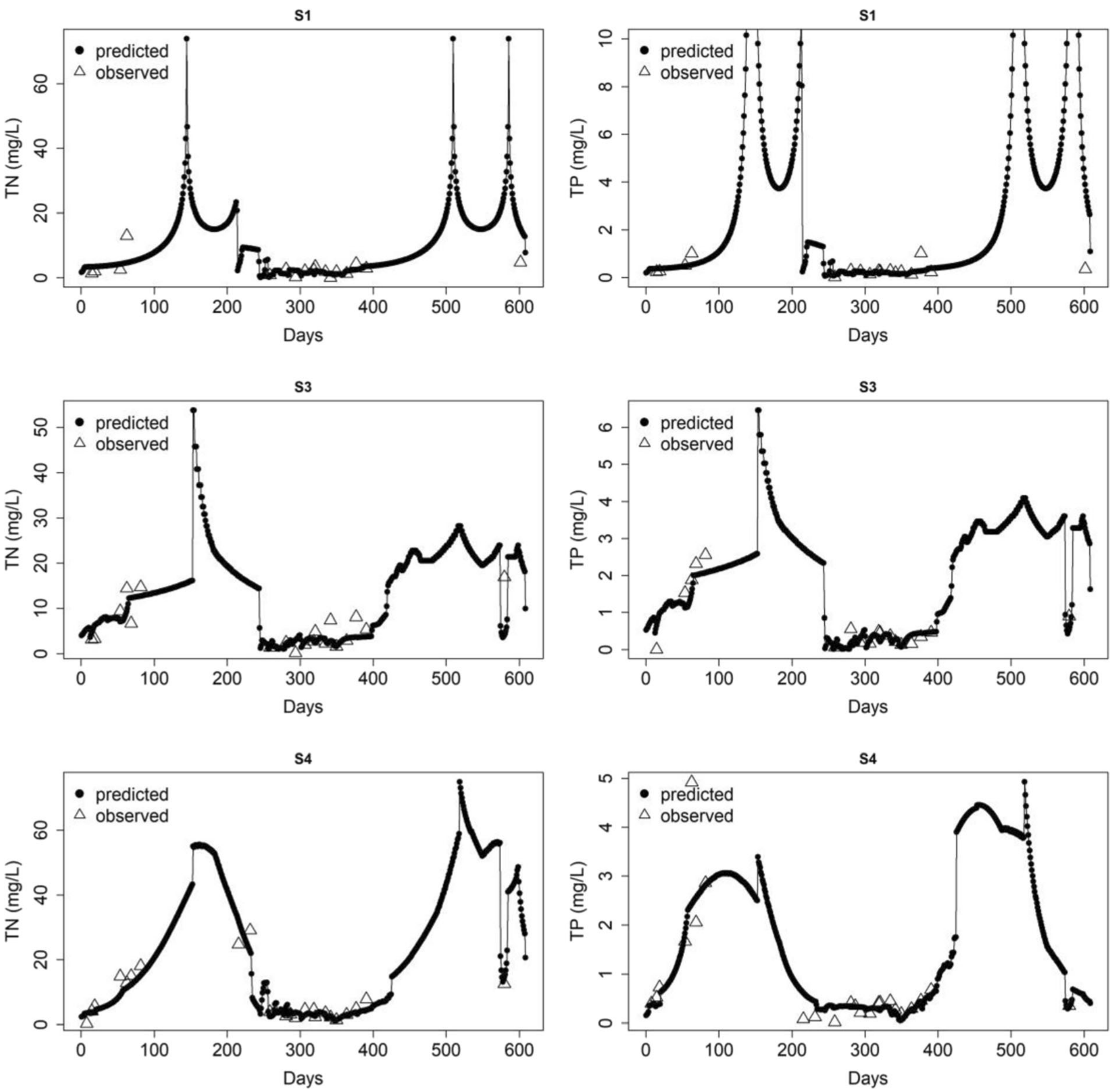

Fig. 2 Comparison of the daily predicted and observed TN and TP concentrations at S1, S3, and S4 for the period between April 1, 2016, and November 30, 2017

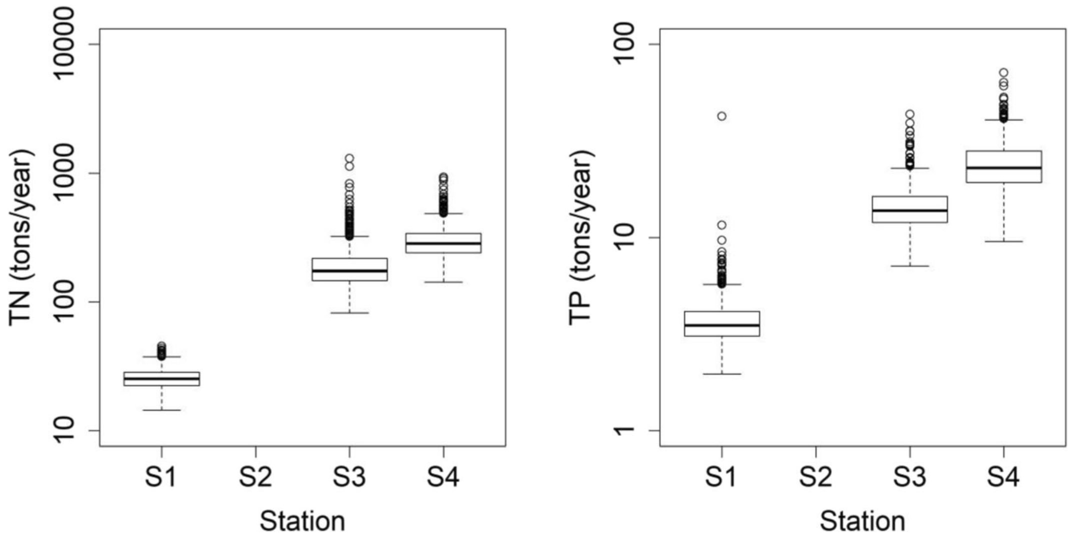

Fig. 3 Predictive regression-based distribution of TN and TP loads at S1, S3, and S4

regression model residuals (Hirsch 2014; Stenback et al. 2011). Given the sparsity of the available water quality monitoring data, it is not possible to assess which of the two approaches produced more accurate and unbiased estimates of loads in our targeted river basin. Increasing the sampling frequency with an emphasis on capturing high discharge events will help to minimize the errors associated with both load estimation methods (Haggard et al. 2003; Lee et al. 2016). Moreover, the variances of each method were found to be statistical different (Levene's test, p value < 0.05), with the exception of TN loads at S3 (Levene's test, p value $= 0.4$). The variance of the TN load using the regression-based method at S4 was higher than that based on the Beale's. This was not the case at S1, where the variability around the load was higher for the Beale's ratio estimate. For TP loads, the Beale's estimated loads were associated with higher variability at S3 and S4.

Nonpoint source loads

The OpenNSPECT estimated total nonpoint TN, TP, and TSS loads reaching the Beirut River at each of the four sampling station are summarized in Table 6. Figure 5 maps the accumulation of the pollutants as they move downstream from the headwaters toward station S4. The accumulated nonpoint TN and TSS loads at S4 and S3 were around 4 times higher than the loads

Table 5 Regression-based flow-concentration models at stations S1, S3, and S4

Station	Regression model equation	Adjusted R^2
S1	$\log(C_{TN}) = 1.29 - 0.47\log(Q)$ $\varepsilon \sim \mathrm{Norm}(0, \sigma^2)$ 0.5728	0.41
	$log(C_{TP}) = -1.6 - 0.53\log(Q)$ $\varepsilon \sim \mathrm{Norm}(0, \sigma^2)$ 0.6551	0.42
S3	$log(C_{TN}) = 1.72 - 0.21\log(Q)$ $\varepsilon \sim \mathrm{Norm}(0, \sigma^2)$ 0.4053	0.29
	$\sqrt[3]{C_{TP}} = 0.84 - 0.16\log(Q)$ $\varepsilon \sim \mathrm{Norm}(0, \sigma^2)$ 0.2064	0.58
S4	$log(C_{TN}) = 2.03 - 0.33\log(Q) - 0.83\cos(2\pi T/365)$ $\varepsilon \sim \mathrm{Norm}(0, \sigma^2)$ 0.6739	0.59
	$\sqrt[3]{C_{TP}} = 0.18 - 0.14\log(Q) - 0.14\sin(2\pi T/365) \times \log(Q)$ $\varepsilon \sim \mathrm{Norm}(0, \sigma^2)$ 0.1869	0.66

estimated at S1. As for TP, the estimated nonpoint loads at S4 and S3 were approximately 3 times higher than the loads at S1. The areas contributing the highest amounts of nonpoint nitrogen and phosphorus loads to the river were mainly found to be the agricultural lands in the headwaters as well as the dense urban areas in the lower sections of the basin. Both of these regions were associated with high effective pollutant concentrations. Moreover, urban and bare lands were also hotspots for the release of TSS, given the high volume of runoff passing through these locations. Table 7 summarizes the nonpoint pollutant loads entering each of the 5 sub-catchments of the Beirut River in tons/km^2/year. Clearly sub-catchments S4B and S5B had the highest nonpoint pollutant loads per km^2. Although these two sub-basins have relatively small areas, their relative contributions to the nonpoint pollution load were high. As a matter of fact, the average nonpoint TN load/km^2/year at SB5 was found to be 2.7 to 3.4 times higher than that of S1B and S2B, respectively. Similarly, the nonpoint TP load/km^2/year at S5B was approximately 2.8 to 4.1 times larger than S1B and S2B, respectively. As for the area-averaged nonpoint TSS loads, the load at S5B was around 2.4 times higher than the loads at S1B and S2B. These findings indicate that the highly urbanized regions (mostly in S5B and S4B) of the basin are contributing the most nonpoint pollutants by area. Note that sub-basin SB1 had the lowest area-averaged load of nonpoint source pollutants; that sub-basin is still dominated with dense forests. Nevertheless, comparing the nonpoint source contributions to the total estimated loads (Table 7), it becomes clear that the nonpoint sources are largely marginal across the entire watershed. This is especially true for the downstream stations where their contribution does not exceed 2.5% of the total annual TP, TN, and TSS loads generated in S3B and S4B. In the headwaters of S1B and S2B, the nonpoint sources were estimated to contribute around 25% of the

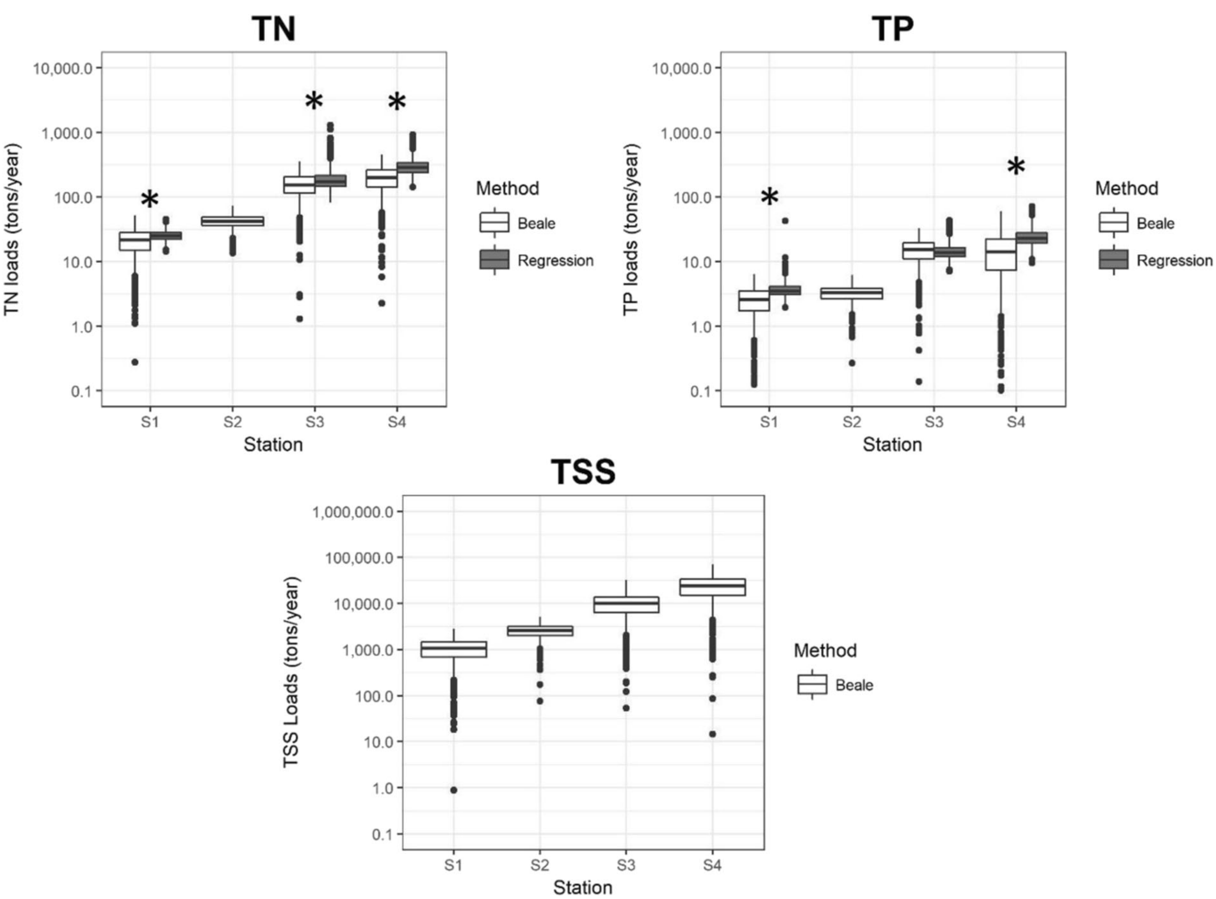

Fig. 4 Comparison between the regression-based and Beale's ratio-based load estimated for TN, TP, and TSS at the four sampling sites. * highlights the estimated loads that were found to statistically differ at the 95% confidence interval between the two methods

Table 6 Pollutant load estimation using the Beale's method

	Total TN load (tons/year)		Total TP load (tons/year)		Total TSS load (tons/year)	
	Mean	SD	Mean	SD	Mean	SD
S1	21.84	9.5	2.60	1.35	1,007.28	1,033.60
S2	42.38	8.96	3.28	0.88	2,538.91	1,364.92
S3	158.41	66.23	14.72	6.22	9,521.33	10,129.08
S4	204.38	86.29	7.97	14.99	23,407.62	25,862.65

total TP loads, 14% of the TN loads, and 10% of the TSS loads.

Overall, the estimated annual area-averaged fluxes of TN (between 0.44 and 11.49 tons of N/km^2/year) and TP (0.03–2.03 tons of P/km^2/year) (Table 8) were considerably higher that the global estimates (0.355 tons of N/km^2/year; 0.001 tons of P/km^2/year) (Harrison et al. 2005; Meybeck et al. 2006; Junior et al. 2018) as well as the estimates for Mediterranean river basins (1.25 tons N/km^2/year and 0.17 tons P/km^2/year) (Vollenweider et al. 1996). This highlights the important role that these relatively small, seasonal, and exorheic watersheds play in the delivery of land-based pollutants to sensitive coastal areas.

The negative impact of increased urbanization on the river water quality of the Beirut River is

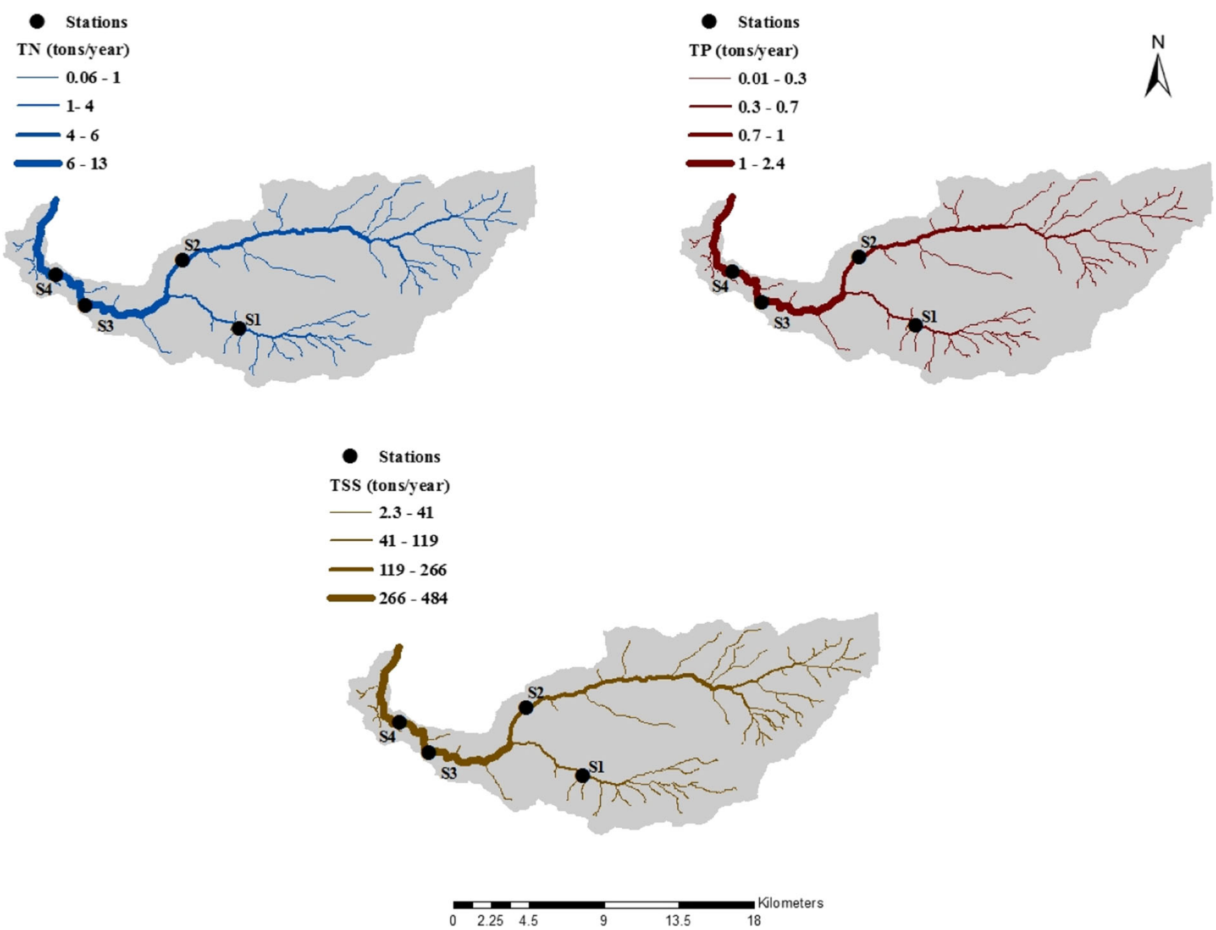

Fig. 5 Spatial distribution of the nonpoint TN, TP, and TSS loads (tons/year) in the basin

Table 7 Nonpoint-based TN, TP, and TSS loads at the four sampling locations over a year

Station	TN (tons/year)	TP (tons/year)	TSS (tons/year)
S1	3.11	0.61	106.31
S2	6.08	1.04	259.68
S3	10.51	1.92	407.36
S4	10.96	2.02	421.61

clearly seen when comparing the estimated area-normalized annual total pollutant loads generated in each sub-basin to its percent urban areas. Annual area-averaged TN loads entering the sparsely populated (low population density) two upper sub-basins, namely, SB1 and SB2, were largely similar (0.44 and 0.34 tons/km^2/year, respectively); however, the annual area-averaged loads emitted within the urbanized SB3 and SB4 were found to be one to two orders of magnitudes larger (2.55 and 11.49 tons/km^2/year, respectively). For TP, the lowest total annual area-average load was identified at S2B (0.03 tons/km^2/year). Downstream at the densely urbanized SB4, the total TP area-averaged load being discharged within the boundaries of the sub-watershed were found to be around 78 times higher than the S2B loads. The spatial loading pattern for TSS was also similar, with TSS area-averaged loads at SB4 more than 170 times larger than the area-averaged total load at S2B. As a matter of fact, the correlation between the percent urban area and the area-averaged annual pollutant loads generated within each sub-catchment was 0.99 for all three pollutants. This strong positive correlation is an indicator that the level of urbanization was a good predictor of the pollutant loads generated at the sub-catchment level. While the negative impact of urbanization on water quality has been shown in many other river basins (Brodie 2013; Chen et al. 2016; Wu and Chen 2013; Chang 2008; Bu et al. 2010; Kamjunke et al. 2013), the dramatic scale of the deterioration observed in the study area is a direct result of the compounded effect that the discharge of untreated domestic and industrial wastewater has on the river. Moreover, the urbanized regions in the basin tend to occur in regions of high slopes, and as such soil erosion is magnified. Given the fast rate of urbanization in the basin, it is expected that future urban growth will further aggravate the water quality issues, particularly that urbanization is occurring in regions where sewerage networks and domestic wastewater treatment plant are either nonexistent, under construction, or not operational. During the study period, high levels of BOD as well as fecal coliforms were recorded along the entire watershed, which highlighted that the discharge of untreated wastewater is not just an urban problem but also an issue in the more rural sections of the basin. Interestingly, the ratio of BOD to COD in the upstream areas was around 0.45, while the lower two stations (SB3 and SB4) had ratios below 0.2. Low BOD to COD ratios in the absence of wastewater treatment plants are often good indicators of industrial wastewater pollution. These findings highlight the pressure that the industrial areas in the lower sections of the basin have on its quality.

Table 8 Summary of mean annual area averaged total and non-point pollutant loads contributed within each sub-catchment

Sub-basin		Area average TN load (Tons/km^2/year)	Area average TP load (Tons/km^2/year)	Area average TSS load (Tons/km^2/year)
S1B	Total:	0.44	0.05	20.56
	Non-point:	0.063	0.012	2.167
S2B	Total:	0.34	0.03	20.15
	Non-point:	0.048	0.008	2.058
S3B	Total:	2.55	0.24	161.49
	Non-point:	0.034	0.006	1.089
S4B	Total:	11.49	2.03	3471.57
	Non-point:	0.146	0.029	4.756
S5B	Total:	NA	NA	NA
	Non-point:	0.162	0.034	5.230

Conclusions and recommendations

This study is the first attempt at generating and apportioning pollution load estimates at the watershed level in Lebanon. The two adopted load estimation methods proved to be robust and capable of providing a transparent quantification of the uncertainties associated with a poorly monitored watershed with a high heterogeneity in its land use/land cover fabric, seasonal flow patterns, and elevation gradients. Further studies are needed to ascertain the suitability, validity, and accuracy of these two load estimation methods in other seasonal Mediterranean rivers. Moreover, the large uncertainties associated with the estimated loads highlight the advantages of adopting high-frequency water quality monitoring in such seasonal rivers, which experience large spatiotemporal variabilities.

The apportionment of pollutant loads between point and nonpoint sources showed that the former was by far the dominant source of pollution to the Beirut River. Among the point sources, the discharge of domestic and industrial wastewater appears to be the leading sources of nutrient and sediment loads reaching the river. As such, there is a need to survey the entire watershed to identify the major domestic and industrial outfalls discharging into the river. There is an urgency to prioritize the implementation of the national wastewater treatment plan that envisions building new wastewater treatment stations within the watershed, as urban areas proved to be the major contributor of pollution. Up until these treatment stations are constructed and made operational, concerned municipalities should control the rate of urbanization in the Beirut River basin. As for the management of the industrial effluents, there is a pressing need to implement the existing laws and regulations and to introduce new mechanisms that adopt the principle of the polluter pays while also providing incentives to encourage industries to manage and reduce their generated wastes and wastewater. With regard to the management of diffused sources, it was clear that the role of the agricultural runoff in the basin is comparatively small. Yet, the high slopes and erodibility of the area highlight the need to implement best management practices all along the river such as establishing riparian buffer zones, encouraging terracing, embracing green infrastructure, managing irrigation and nutrient application, as well as using soil erosion control measures. Lastly, the quantification and valuation of the ecosystem service that are provided by the forested areas in the basin with regard to reducing pollution levels should be initiated with the hope that such this efforts will help increase the awareness of the public and reduce increased deforestation within the basin.

Funding information This study was made possible through the generous support of the American University of Beirut's Research Board (Award No.: 103008; Project No.: 22713).

References

Akaike, H. (1974). A new look at the statistical model identification. *IEEE Transactions on Automatic Control, 19*, 716–723.

Alameddine, I., Qian, S. S., & Reckhow, K. H. (2011). A Bayesian changepoint–threshold model to examine the effect of TMDL implementation on the flow–nitrogen concentration relationship in the Neuse River basin. *Water Research, 45*(1), 51–62.

Alberto, W. D., del Pilar, D. M., Valeria, A. M., Fabiana, P. S., Cecilia, H. A., & de los Ángeles, B. M. (2001). Pattern recognition techniques for the evaluation of spatial and temporal variations in water quality. A case study: Suquía River Basin (Córdoba–Argentina). *Water Research, 35*(12), 2881–2894.

Alberto, A., St-Hilaire, A., Courtenay, S. C., & Van Den Heuvel, M. R. (2016). Monitoring stream sediment loads in response to agriculture in Prince Edward Island, Canada. *Environmental Monitoring and Assessment, 188*(7), 415.

Auerbach, D. A., Deisenroth, D. B., McShane, R. R., McCluney, K. E., & LeRoy Poff, N. (2014). Beyond the concrete: accounting for ecosystem services from free-flowing rivers. *Ecosystem Services, 10*, 1–5. https://doi.org/10.1016/j.ecoser.2014.07.005.

Balter, M. (2013). Archaeologists say the 'Anthropocene' is here—but it began long ago. *Science, 340*(6130), 261–262.

Bernal, S., von Schiller, D., Sabater, F., & Martí, E. (2013). Hydrological extremes modulate nutrient dynamics in Mediterranean climate streams across different spatial scales. *Hydrobiologia, 719*(1), 31–42.

Borja, A., Galparsoro, I., Solaun, O., Muxika, I., Tello, E. M., Uriarte, A., et al. (2006). The European Water Framework Directive and the DPSIR, a methodological approach to assess the risk of failing to achieve good ecological status. *Estuarine, Coastal and Shelf Science, 66*(1–2), 84–96.

Bowes, M. J., Smith, J. T., Jarvie, H. P., & Neal, C. (2008). Modelling of phosphorus inputs to rivers from diffuse and point sources. *Science of the Total Environment, 395*(2–3), 125–138.

Brezonik, P. L., & Stadelmann, T. H. (2002). Analysis and predictive models of stormwater runoff volumes, loads, and pollutant concentrations from watersheds in the twin cities metropolitan area, Minnesota, USA. *Water Research, 36*(7), 1743–1757.

Brodie, J. E. (2013). *2013 scientific consensus statement: land use impacts on the great barrier reef water quality and ecosystem condition*: reef water quality protection plan secretariat.

Bu, H., Tan, X., Li, S., & Zhang, Q. (2010). Temporal and spatial variations of water quality in the Jinshui River of the South Qinling Mts., China. *Ecotoxicology and Environmental Safety, 73*(5), 907–913.

Carpenter, S. R., Stanley, E. H., & Vander Zanden, M. J. (2011). State of the world's freshwater ecosystems: physical, chemical, and biological changes. *Annual Review of Environment and Resources, 36*, 75–99.

Cha, Y., Stow, C. A., Reckhow, K. H., DeMarchi, C., & Johengen, T. H. (2010). Phosphorus load estimation in the Saginaw River, MI using a Bayesian hierarchical/multilevel model. *Water Research, 44*(10), 3270–3282. https://doi.org/10.1016/j.watres.2010.03.008.

Chang, H. (2008). Spatial analysis of water quality trends in the Han River basin, South Korea. *Water Research, 42*(13), 3285–3304.

Chapman, D. V. (1996). *Water quality assessments: a guide to the use of biota, sediments, and water in environmental monitoring* (2nd ed.). London: E & FN Spon.

Chen, D., Hu, M., Wang, J., Guo, Y., & Dahlgren, R. A. (2016). Factors controlling phosphorus export from agricultural/forest and residential systems to rivers in eastern China, 1980–2011. *Journal of Hydrology, 533*, 53–61.

Cohn, T. A. (1995). Recent advances in statistical methods for the estimation of sediment and nutrient transport in rivers. *Reviews of Geophysics, 33*(S2), 1117–1123.

Cohn, T. A., Delong, L. L., Gilroy, E. J., Hirsch, R. M., & Wells, D. K. (1989). Estimating constituent loads. *Water Resources Research, 25*(5), 937–942.

Da Silva, A. M. M., & Sacomani, L. B. (2001). Using chemical and physical parameters to define the quality of Pardo River water (Botucatu-SP-Brazil). *Water Research, 35*(6), 1609–1616.

Darwish, T. (2006). *Soil map of Lebanon: 1:50 000*. Beirut: Lebanese National Council for Scientific Research. Remote Sensing, Remote Sensing Center.

Diaz, R. J. (2001). Overview of hypoxia around the world. *Journal of Environmental Quality, 30*(2), 275–281.

Ding, X., Shen, Z., Liu, R., Chen, L., & Lin, M. (2014). Effects of ecological factors and human activities on nonpoint source pollution in the upper reach of the Yangtze River and its management strategies. *Hydrology and Earth System Sciences Discussions, 11*(1), 691–721.

Dolan, D. M., Yui, A. K., & Geist, R. D. (1981). Evaluation of river load estimation methods for total phosphorus. *Journal of Great Lakes Research, 7*(3), 207–214.

Efthimiou, N. (2019). The role of sediment rating curve development methodology on river load modeling. *Environmental Monitoring and Assessment, 191*(2), 108.

El-Nakib, S., Alameddine, I., Abou Najm, M., & Massoud, M. (*2018*). Quantifying the spatio-temporal variability of water quality in an urbanizing perennial Mediterranean river: the case of the Beirut River. In S. Hernández & S. Mambretti (Eds.), *Water Pollution XIV, A Coruña, Spain* (Vol. 228, pp. 187–197). WIT Transactions on Ecology and the Environment.

Elwan, A., Singh, R., Patterson, M., Roygard, J., Horne, D., Clothier, B., & Jones, G. (2018). Influence of sampling frequency and load calculation methods on quantification of annual river nutrient and suspended solids loads. *Environmental Monitoring and Assessment, 190*(2), 78.

Ferguson, R. (1986). River loads underestimated by rating curves. *Water Resources Research, 22*(1), 74–76.

Ferguson, R. (1987). Accuracy and precision of methods for estimating river loads. *Earth Surface Processes and Landforms, 12*(1), 95–104.

Gelman, A., Su, Y.-S., Yajima, M., Hill, J., Pittau, M. G., & Kerman, J. (2016). Arm: data analysis using regression and multilevel/hierarchical models. 2015. *URL https://CRAN.R-project.org/package=arm*. R package version, 1.9–3.

Gilroy, E., Hirsch, R., & Cohn, T. (1990). Mean square error of regression-based constituent transport estimates. *Water Resources Research, 26*(9), 2069–2077.

Granger, S., Bol, R., Anthony, S., Owens, P., White, S., & Haygarth, P. (2010). Towards a holistic classification of diffuse agricultural water pollution from intensively managed grasslands on heavy soils. In *Advances in Agronomy* (Vol. 105, pp. 83–115). Elsevier.

Grizzetti, B., Bouraoui, F., De Marsily, G., & Bidoglio, G. (2005). A statistical method for source apportionment of riverine nitrogen loads. *Journal of Hydrology, 304*(1–4), 302–315.

Haggard, B., Soerens, T., Green, W., & Richards, R. (2003). Using regression methods to estimate stream phosphorus loads at the Illinois River, Arkansas. *Applied Engineering in Agriculture, 19*(2), 187.

Harmel, R., & King, K. (2005). Uncertainty in measured sediment and nutrient flux in runoff from small agricultural watersheds. *Transactions of ASAE, 48*(5), 1713–1721.

Harrison, J. A., Seitzinger, S. P., Bouwman, A., Caraco, N. F., Beusen, A. H., & Vörösmarty, C. J. (2005). Dissolved inorganic phosphorus export to the coastal zone: results from a spatially explicit, global model. *Global Biogeochemical Cycles, 19*(4).

Hirsch, R. M. (2014). Large biases in regression-based constituent flux estimates: causes and diagnostic tools. *JAWRA Journal of the American Water Resources Association, 50*(6), 1401–1424.

Hirsch, R. M., Moyer, D. L., & Archfield, S. A. (2010). Weighted regressions on time, discharge, and season (WRTDS), with an application to Chesapeake Bay river inputs 1. *JAWRA Journal of the American Water Resources Association, 46*(5), 857–880.

Jomaa, S., Aboud, I., Dupas, R., Yang, X., Rozemeijer, J., & Rode, M. (2018). Improving nitrate load estimates in an agricultural catchment using event response reconstruction. *Environmental Monitoring and Assessment, 190*(6), 330.

Junior, F. T., Lima, A., & Barroso, G. (2018). Emission rates of nitrogen and phosphorus in a tropical coastal river basin: a strategic management approach. *Environmental Monitoring and Assessment, 190*(12), 747.

Kalogianni, E., Vourka, A., Karaouzas, I., Vardakas, L., Laschou, S., & Skoulikidis, N. T. (2017). Combined effects of water stress and pollution on macroinvertebrate and fish assemblages in a Mediterranean intermittent river. *Science of the Total Environment, 603*, 639–650.

Kamjunke, N., Büttner, O., Jäger, C. G., Marcus, H., von Tümpling, W., Halbedel, S., Norf, H., Brauns, M., Baborowski, M., Wild, R., Borchardt, D., & Weitere, M. (2013). Biogeochemical patterns in a river network along a land use gradient. *Environmental Monitoring and Assessment, 185*(11), 9221–9236.

Karydis, M., & Kitsiou, D. (2012). Eutrophication and environmental policy in the Mediterranean Sea: a review. *Environmental Monitoring and Assessment, 184*(8), 4931–4984.

KBAC (2007). Ko'olaupoko watershed restoration action strategy. Hawai'i's Department of Health: Kailua Bay advisory council (KBAC).

Koch, R. W., & Smillie, G. M. (1986). Bias in hydrologic prediction using log-transformed regression models. *JAWRA Journal of the American Water Resources Association, 22*(5), 717–723.

Lee, C. J., Hirsch, R. M., Schwarz, G. E., Holtschlag, D. J., Preston, S. D., Crawford, C. G., et al. (2016). An evaluation of methods for estimating decadal stream loads. *Journal of Hydrology, 542*, 185–203.

Littlewood, I. (1995). Hydrological regimes, sampling strategies, and assessment of errors in mass load estimates for United Kingdom rivers. *Environment International, 21*(2), 211–220.

Littlewood, I., & Marsh, T. (2005). Annual freshwater river mass loads from Great Britain, 1975–1994: estimation algorithm, database and monitoring network issues. *Journal of Hydrology, 304*(1–4), 221–237.

Littlewood, I., Watts, C., & Custance, J. (1998). Systematic application of United Kingdom river flow and quality databases for estimating annual river mass loads (1975–1994). *Science of the Total Environment, 210*, 21–40.

López-Doval, J. C., Ginebreda, A., Caquet, T., Dahm, C. N., Petrovic, M., Barceló, D., et al. (2013). Pollution in Mediterranean-climate rivers. *Hydrobiologia, 719*(1), 427–450.

Malagó, A., Bouraoui, F., Grizzetti, B., & De Roo, A. (2019). Modelling nutrient fluxes into the Mediterranean Sea. *Journal of Hydrology: Regional Studies, 22*, 100592.

Malan, H., & Day, J. (2003). Linking flow, water quality and potential effects on aquatic biota within the reserve determination process. *Water SA, 29*(3), 297–304.

Massoud, M. A., El-Fadel, M., Scrimshaw, M. D., & Lester, J. N. (2006). Factors influencing development of management strategies for the Abou Ali River in Lebanon II: seasonal and annual variation. *Science of the Total Environment, 362*(1–3), 31–41.

Meybeck, M. (2003). Global analysis of river systems: from Earth system controls to Anthropocene syndromes. *Philosophical Transactions of the Royal Society, B: Biological Sciences, 358*(1440), 1935–1955.

Meybeck, M., Dürr, H. H., & Vörösmarty, C. J. (2006). Global coastal segmentation and its river catchment contributors: a new look at land-ocean linkage. *Global Biogeochemical Cycles, 20*(1).

Moatar, F., & Meybeck, M. (2005). Compared performances of different algorithms for estimating annual nutrient loads discharged by the eutrophic river Loire. *Hydrological Processes: An International Journal, 19*(2), 429–444.

Moatar, F., Person, G., Meybeck, M., Coynel, A., Etcheber, H., & Crouzet, P. (2006). The influence of contrasting suspended particulate matter transport regimes on the bias and precision of flux estimates. *Science of the Total Environment, 370*(2–3), 515–531.

Mockler, E. M., Deakin, J., Archbold, M., Daly, D., & Bruen, M. (*2016*). Nutrient load apportionment to support the identification of appropriate water framework directive measures. In *Biology and Environment: Proceedings of the Royal Irish Academy* (Vol. 116, pp. 245–263, Vol. 3). JSTOR.

Morrison, K. D., & Kolden, C. A. (2015). Modeling the impacts of wildfire on runoff and pollutant transport from coastal watersheds to the nearshore environment. *Journal of Environmental Management, 151*, 113–123.

National Research Council. (2001). *Assessing the TMDL approach to water quality management*. Washington D.C.: National Academies Press.

NOAA (2012). Tutorial for OpenNSPECT, version 1.1: example analyses for the Waianae Region of Oahu, Hawaii. National Oceanic and Atmospheric Administration (NOAA) coastal services center.

NOAA (2014). Technical guide for OpenNSPECT, version 1.2. National Oceanic and Atmospheric Administration (NOAA) coastal services center.

Novotny, V. (1999). Integrating diffuseinonpoint pollution control and water body restoration into watershed management. *JAWRA Journal of the American Water Resources Association, 35*(4), 717–727.

Novotny, V. (2003). *Water quality: Diffuse pollution and watershed management*. Hoboken: Wiley.

Park, Y. S., & Engel, B. A. (2014). Use of pollutant load regression models with various sampling frequencies for annual load estimation. *Water, 6*(6), 1685–1697.

Pellerin, B. A., Bergamaschi, B. A., Gilliom, R. J., Crawford, C. G., Saraceno, J., Frederick, C. P., Downing, B. D., & Murphy, J. C. (2014). Mississippi River nitrate loads from high frequency sensor measurements and regression-based load estimation. *Environmental Science & Technology, 48*(21), 12612–12619.

Phillips, J., Webb, B., Walling, D., & Leeks, G. (1999). Estimating the suspended sediment loads of rivers in the LOIS study area using infrequent samples. *Hydrological Processes, 13*(7), 1035–1050.

Preston, S. D., Bierman, V. J., & Silliman, S. E. (1989). An evaluation of methods for the estimation of tributary mass loads. *Water Resources Research, 25*(6), 1379–1389.

Qian, S. S. (2016). *Environmental and ecological statistics with R* (2ed., Chapman & Hall/CRC applied environmental statistics). Boca Ratan, FL.: Chapman and hall/CRC.

Quilbé, R., Rousseau, A. N., Duchemin, M., Poulin, A., Gangbazo, G., & Villeneuve, J.-P. (2006). Selecting a calculation method to estimate sediment and nutrient loads in streams: application to the Beaurivage River (Québec, Canada). *Journal of Hydrology, 326*(1–4), 295–310.

R Core Team (2017). R: A language and environment for statistical computing. In R. D. C. Team (Ed.), R Foundation for Statistical Computing. Vienna: R Foundation for statistical computing.

Rabalais, N. N., Turner, R. E., Díaz, R. J., & Justić, D. (2009). Global change and eutrophication of coastal waters. *ICES Journal of Marine Science, 66*(7), 1528–1537.

Reinelt, L. E., & Grimvall, A. (1992). Estimation of nonpoint source loadings with data obtained from limited sampling programs. *Environmental Monitoring and Assessment, 21*(3), 173–192.

Rice, E. W., Bridgewater, L., Water Environment, F., American Water Works, A., & American Public Health, A. (2012). *Standard methods for the examination of water and* *wastewater* (Vol. 22nd, Vol. Book, Whole). Washington, D.C: American Public Health Association.

Richards, R. P. (1998). Estimation of pollutant loads in rivers and streams: a guidance document for NPS programs. *Project report prepared under Grant X998397-01-0, US Environmental Protection Agency, Region VIII, Denver*, 108.

Richards, R. P., & Holloway, J. (1987). Monte Carlo studies of sampling strategies for estimating tributary loads. *Water Resources Research, 23*(10), 1939–1948.

Rissman, A. R., & Carpenter, S. R. (2015). Progress on nonpoint pollution: Barriers & opportunities. *Daedalus, 144*(3), 35–47.

Rozemeijer, J. C., Van der Velde, Y., Van Geer, F. C., De Rooij, G. H., Torfs, P. J., & Broers, H. P. (2010). Improving load estimates for NO3 and P in surface waters by characterizing the concentration response to rainfall events. *Environmental Science & Technology, 44*(16), 6305–6312.

Runkel, R. L., Crawford, C. G., & Cohn, T. A. (2004). Load estimator (LOADEST): A FORTRAN program for estimating constituent loads in streams and rivers.

Salles, C., Tournoud, M. G., & Chu, Y. (2008). Estimating nutrient and sediment flood loads in a small Mediterranean river. *Hydrological Processes: An International Journal, 22*(2), 242–253.

Scavia, D., & Bricker, S. B. (2006). Coastal eutrophication assessment in the United States. In *nitrogen cycling in the Americas: natural and anthropogenic influences and controls* (pp. 187–208). Springer.

Schoumans, O., Chardon, W., Bechmann, M., Gascuel-Odoux, C., Hofman, G., Kronvang, B., et al. (2014). Mitigation options to reduce phosphorus losses from the agricultural sector and improve surface water quality: a review. *Science of the Total Environment, 468*, 1255–1266.

Smith, C., & Croke, B. (2005). Sources of uncertainty in estimating suspended sediment load. *IAHS-AISH publication*, 136-143.

Srinivasan, R., & Arnold, J. G. (1994). Integration of a basin-scale water quality model with GIS. *Journal of the American Water Resources Association, 30*(3), 453–462.

Stenback, G. A., Crumpton, W. G., Schilling, K. E., & Helmers, M. J. (2011). Rating curve estimation of nutrient loads in Iowa rivers. *Journal of Hydrology, 396*(1–2), 158–169.

Strayer, D. L., Beighley, R. E., Thompson, L. C., Brooks, S., Nilsson, C., Pinay, G., et al. (2003). Effects of land cover on stream ecosystems: roles of empirical models and scaling issues. *Ecosystems, 6*(5), 407–423.

Tappin, A. D., Mankasingh, U., McKelvie, I. D., & Worsfold, P. J. (2013). Temporal variability in nutrient concentrations and loads in the river Tamar and its catchment (SW England) between 1974 and 2004. *Environmental Monitoring and Assessment, 185*(6), 4791–4818.

Tin, M. (1965). Comparison of some ratio estimators. *Journal of the American Statistical Association, 60*(309), 294–307. https://doi.org/10.1080/01621459.1965.10480792.

Turner, R. E., & Rabalais, N. N. (2003). Linking landscape and water quality in the Mississippi River basin for 200 years. *Bioscience, 53*(6), 563–572.

Tzoraki, O., Nikolaidis, N. P., Cooper, D., & Kassotaki, E. (2014). Nutrient mitigation in a temporary river basin. *Environmental Monitoring and Assessment, 186*(4), 2243–2257.

Ullrich, A., & Volk, M. (2010). Influence of different nitrate–N monitoring strategies on load estimation as a base for model calibration and evaluation. *Environmental Monitoring and Assessment, 171*(1–4), 513–527.

UN (2003). Water: A Matter of Life and Death. Fact sheet. International Year of Freshwater 2003: United Nations.

USEPA (2000). Ambient water quality criteria recommendations: information supporting the development of state and tribal nutrient criteria for rivers and streams in nutrient Ecoregion III: Xeric west. In O. o. W. a. O. o. S. a. Technology (Ed.). Washington, D.C.: United States Environmental Protection Agency.

Vandenberghe, V., Goethals, P., Van Griensven, A., Meirlaen, J., De Pauw, N., Vanrolleghem, P., et al. (2005). Application of automated measurement stations for continuous water quality monitoring of the Dender River in Flanders, Belgium. *Environmental Monitoring and Assessment, 108*(1–3), 85–98.

Vega, M., Pardo, R., Barrado, E., & Debán, L. (1998). Assessment of seasonal and polluting effects on the quality of river water by exploratory data analysis. *Water Research, 32*(12), 3581–3592.

Viswanathan, C., & Karim, M. (*2015*). Non point source pollution modeling using NSPECT model to facilitate watershed planning. In *World Environmental and Water Resources Congress 2015* (pp. 2599–2606).

Vollenweider, R. A., Rinaldi, A., Viviani, R., & Todini, E. (1996). Assessment of the state of eutrophication in the Mediterranean Sea. In UNEP (Ed.). Athens: *MAP Technical Reports Series*.

Vörösmarty, C. J., Lévêque, C., Revenga, C., Bos, R., Caudill, C., Chilton, J., et al. (2005). Fresh water. *Millennium ecosystem assessment, 1*, 165–207.

Vörösmarty, C. J., McIntyre, P. B., Gessner, M. O., Dudgeon, D., Prusevich, A., Green, P., et al. (2010). Global threats to human water security and river biodiversity. *Nature, 467*(7315), 555–561.

Wang, Y., He, B., Duan, W., Li, W., Luo, P., & Razafindrabe, B. H. N. (2016). Source apportionment of annual water pollution loads in river basins by remote-sensed land cover classification. *Water, 8*(9), 361.

Wu, Y., & Chen, J. (2013). Investigating the effects of point source and nonpoint source pollution on the water quality of the East River (Dongjiang) in South China. *Ecological Indicators, 32*, 294–304.

Yang, Y., & Wang, L. (2010). A review of modelling tools for implementation of the EU water framework directive in handling diffuse water pollution. *Water Resources Management, 24*(9), 1819–1843.

Publisher's note Springer Nature remains neutral with regard to jurisdictional claims in published maps and institutional affiliations.